Unraveling the immunological landscape and gut microbiome in sepsis: a comprehensive approach to diagnosis and prognosis

Yali Luo,[a] Jian Gao,[a] Xinliang Su,[a] Helian Li,[a] Yingcen Li,[a] Wenhao Qi,[a] Xuling Han,[a] Jingxuan Han,[a] Yiran Zhao,[a] Alin Zhang,[a] Yan Zheng,[a,b,***] Feng Qian,[a,b,**] and Hongyu He[c,*]

[a]State Key Laboratory of Genetic Engineering, Human Phenome Institute, School of Life Sciences, Zhangjiang Fudan International Innovation Center, Fudan University, Shanghai, 200433, China
[b]Ministry of Education Key Laboratory of Contemporary Anthropology, School of Life Sciences, Fudan University, Shanghai, 200438, China
[c]Department of Critical Care Medicine, Zhongshan Hospital, Fudan University, Shanghai, 200032, China

eBioMedicine
2025;113: 105586
Published Online xxx
https://doi.org/10.1016/j.ebiom.2025.105586

Summary

Background Comprehensive and in-depth research on the immunophenotype of septic patients remains limited, and effective biomarkers for the diagnosis and treatment of sepsis are urgently needed in clinical practice.

Methods Blood samples from 31 septic patients in the Intensive Care Unit (ICU), 25 non-septic ICU patients, and 18 healthy controls were analyzed using flow cytometry for deep immunophenotyping. Metagenomic sequencing was performed in 41 fecal samples, including 13 septic patients, 10 non-septic ICU patients, and 18 healthy controls. Immunophenotype shifts were evaluated using differential expression sliding window analysis, and random forest models were developed for sepsis diagnosis or prognosis prediction.

Findings Septic patients exhibited decreased proportions of natural killer (NK) cells and plasmacytoid dendritic cells (pDCs) in $CD45^+$ leukocytes compared with non-septic ICU patients and healthy controls. These changes statistically mediated the association of *Bacteroides salyersiae* with sepsis, suggesting a potential underlying mechanism. A combined diagnostic model incorporating *B.salyersia*, NK cells in $CD45^+$ leukocytes, and C-reactive protein (CRP) demonstrated high accuracy in distinguishing sepsis from non-sepsis (area under the receiver operating characteristic curve, AUC = 0.950, 95% CI: 0.811–1.000). Immunophenotyping and disease severity analysis identified an Acute Physiology and Chronic Health Evaluation (APACHE) II score threshold of 21, effectively distinguishing mild (n = 19) from severe (n = 12) sepsis. A prognostic model based on the proportion of total lymphocytes, Helper T (Th) 17 cells, $CD4^+$ effector memory T (T_{EM}) cells, and Th1 cells in $CD45^+$ leukocytes achieved robust outcome prediction (AUC = 0.906, 95% CI: 0.732–1.000), with further accuracy improvement when combined with clinical scores (AUC = 0.938, 95% CI: 0.796–1.000).

Interpretation NK cell subsets within innate immunity exhibit significant diagnostic value for sepsis, particularly when combined with *B. salyersiae* and CRP. In addition, T cell phenotypes within adaptive immunity are correlated with sepsis severity and may serve as reliable prognostic markers.

Funding This project was supported by the National Key R&D Program of China (2023YFC2307600, 2021YFA1301000), Shanghai Municipal Science and Technology Major Project (2023SHZDZX02, 2017SHZDZX01), Shanghai Municipal Technology Standards Project (23DZ2202600).

Keywords: Sepsis; Immunophenotype; Gut microbiome; Diagnosis; Prognosis

*Corresponding author.
**Corresponding author. State Key Laboratory of Genetic Engineering, Human Phenome Institute, School of Life Sciences, Zhangjiang Fudan International Innovation Center, Fudan University, Shanghai, 200433, China.
***Corresponding author. State Key Laboratory of Genetic Engineering, Human Phenome Institute, School of Life Sciences, Zhangjiang Fudan International Innovation Center, Fudan University, Shanghai, 200433, China.
E-mail addresses: he.hongyu@zs-hospital.sh.cn (H. He), fengqian@fudan.edu.cn (F. Qian), yan_zheng@fudan.edu.cn (Y. Zheng).

Research in context

Evidence before this study

Diagnosing and prognosticating sepsis in clinical practice remains challenging due to the high heterogeneity among septic patients. Previous studies have identified immune dysregulation and alterations in gut microbiome as potential factors influencing sepsis outcomes. However, comprehensive studies integrating both immunophenotyping and gut microbiome analysis to understand their combined impact on sepsis diagnosis and prognosis are limited.

Added value of this study

Our study integrated advanced 11-color flow cytometry and metagenomic sequencing to deliver a comprehensive analysis of the immunological landscape and gut microbiome in septic patients. We identified significant alterations in immune cell subsets, particularly natural killer (NK) cells and plasmacytoid dendritic cells (pDCs), which potentially mediated the relationship between *Bacteroides salyersiae* and sepsis. *B. salyersiae*, along with NK cells and C-reactive protein (CRP), were identified as valuable diagnostic markers for sepsis. In addition, we identified specific T cell subsets within adaptive immunity that correlated with disease severity and predicted patient outcomes when integrated with clinical scores.

Implications of all the available evidence

Our findings, combined with existing evidence, underscore the importance of integrating immune and gut microbiome analyses in sepsis management. By identifying key immune markers and microbiome profiles, clinicians can more accurately stratify patients and tailor interventions, potentially improving outcomes and reducing mortality in sepsis.

Introduction

Sepsis is a life-threatening systemic infection characterized by a dysregulated host response to infection, resulting in multiple organ dysfunction and potential mortality.[1,2] However, despite the gravity of this disease, diagnosing it remains a complex challenge due to its variable presentation and the intricacies of the host's immune response. In 2017, an estimated 48.9 million incident cases of sepsis were reported globally, with approximately 11 million deaths, representing 19.7 percent of all global deaths.[3] This staggering statistic underscores the urgency in refining diagnostic methods and prognostic tools. Although the immune system plays a crucial role in the host's defense against pathogens, its over-activation paradoxically worsens the disease.[4] Pathogen replication within the bloodstream results in the release of toxins and inflammatory cytokines, which, in excessive amounts, may lead to tissue injury and organ dysfunction, even though they initially assist in containing the infection.[4,5] A thorough understanding of the immunological disturbance in patients with sepsis is indispensable for updating effective diagnostic and prognostic strategies.

Sepsis is closely linked to the host immune response, as it is caused by an uncontrolled inflammatory reaction to infection.[6] The immune response in sepsis is complex: concurrent hyper-inflammation and immune suppression affect various cell types and organ systems. Moreover, the host immune state can change at different stages of the disease, including the pivotal role of immune subsets in modulating the systemic immune response.[7–9] For example, the research conducted by Ahmed et al. elucidated that the $CD45^+$ leukocytes are modulated during sepsis in a manner that is both cell-type-specific and stimulus-dependent.[10] These immune alterations serve as potential diagnostic markers, enabling clinicians to distinguish sepsis from other critical conditions in Intensive Care Unit (ICU) patients and therefore facilitating earlier diagnosis.

Recent research has expanded our understanding of sepsis pathogenesis beyond traditional immunological frameworks. A Mendelian randomization study highlighted the potential regulatory role of the gut microbiome by revealing a bidirectional association between gut microbiota composition and sepsis risk.[11] While specific bacterial taxa have been statistically associated with sepsis, the interactions between the gut microbiome and the immune system may influence both disease development and progression. Research has shown that dysbiosis, or an imbalance in the gut microbiota, can worsen sepsis by increasing toxin production, amplifying the inflammatory response, and compromising intestinal barrier function.[12] Furthermore, these microorganisms produce metabolites, such as short-chain fatty acids, that modulate immune cell activity and can influence them through receptor interactions.[13] Therefore, investigating the interplay between microbiota and the immune system may facilitate the identification of new biomarkers and therapeutic targets.

To advance sepsis treatment, a deeper understanding of the immunological mechanisms underlying the condition is crucial. A 2023 review by Cajander et al. in Lancet Respiratory Medicine emphasized the importance of profiling the dysregulated immune response in sepsis.[14] Particularly, blood transcriptomics, proved by emerging evidence, has greatly enhanced our understanding of the host's immune response in sepsis by suggesting the association between distinct blood transcriptional patterns and different clinical outcomes in septic patients. This molecular-level understanding largely complements current clinical practice that relies heavily on disease severity scores such as Sequential Organ Failure Assessment (SOFA) and Acute

Physiology and Chronic Health Evaluation (APACHE) II for prognostic evaluation. Actually, these severity scores cannot fully predict patient outcomes alone. Clinical observations reveal a discrepancy between these scores and patient prognosis: some patients with lower scores but impaired immunity still experience mortality, while younger patients with stronger immunity, when given appropriate treatment, may survive despite higher SOFA scores at ICU admission. This discrepancy highlights that the mechanisms associated with prognosis in septic patients remains underexplored. By identifying markers that accurately reflect immune status, clinicians may better assess a patient's capacity to contain infection and determine their prognosis.

The present study aims to address the aforementioned research gap by examining the immune responses in septic patients. Traditional immunological assessment methods provide a limited view of a patient's immune function because they often fail to capture the full spectrum of immune responses. Therefore, we will employ six advanced 11-color flow cytometry panels to comprehensively evaluate the innate and adaptive immune responses in septic patients. By doing so, we aim to uncover immune markers with the potential for clinical diagnosis and prognosis prediction by deep immunophenotyping. In addition, we further incorporated metagenomic to preliminarily investigate the potential regulatory mechanisms of sepsis immune phenotype, thereby offering new scientific foundations and strategies for diagnosing and treating sepsis.

Methods

Participants

This study is a prospective observational investigation conducted in the ICU of Zhongshan Hospital, Fudan University, from 2022 to 2023. The diagnosis of sepsis was based on the Sepsis 3.0 definition,[1] and all patients were 18 years of age or older. To minimize the influence of critical illness and the ICU environment, the non-septic ICU group consisted of critically ill patients admitted to the ICU for conditions not meeting the diagnostic criteria for sepsis, such as major surgery, hemorrhagic or cardiogenic shock, cerebral hemorrhage/stroke, seizures, and other non-septic critical illnesses. Demographic factors, including age, sex, and body mass index (BMI), were balanced between the sepsis and non-sepsis groups to ensure comparability. Both groups had similar APACHE II scores, indicating comparable severity of illness. Furthermore, ICU patients with conditions that could confound immunophenotypic analysis, such as organ or bone marrow transplantation, high-dose corticosteroid treatment, or autoimmune diseases, were excluded from the study. Healthy participants were recruited from visitors attending the Health Examination Center.

Sample collection and clinical parameter acquisition

Peripheral blood was collected from all participants, with clinical data abstracted from electronic medical records for inpatients. APACHE II scores were calculated from data gathered within the first 48 h of ICU admission. Blood samples from both sepsis and non-sepsis groups were collected within 48 h of ICU admission, and fecal samples were obtained before antibiotic administration when available; if the patient did not have a bowel movement before antibiotic administration, the fecal sample was considered missing. Healthy participants provided both blood and fecal samples. Clinical and demographic data were collected at enrollment. Patient survival vs. mortality was followed for 28 days after entry into the study or until hospital discharge, whichever occurred first.

Sample preservation

Peripheral blood was collected in sodium heparin tubes (BD, catalog no. 367874) and processed within 24 h at room temperature. Fecal samples, collected from ICU patients (both sepsis and non-sepsis) and healthy controls, were stored immediately at –80 °C until processing.

Blood sample treatment

Six standardized 11-color flow cytometry panels were developed to perform deep immunophenotyping of human whole blood.[12] The details were as follows:

Panel design for flow cytometry

Innate immune cell subsets were identified in panel 1, including neutrophils ($CD15^+$ $CD16^+$), eosinophils ($CD15^+$ $CD16^-$), basophils ($lineage^-$ $HLADR^-$ $CD123^+$), myeloid dendritic cells (mDCs, $lineage^-$ $HLADR^+CD11c^{high}$ $CD123^{-/low}$), plasmacytoid dendritic cells (pDCs, $lineage^-$ $HLADR^+$ $CD11c^-$ $CD123^{high}$), classical monocytes ($CD14^{high}$ $CD16^-$), intermediate monocytes ($CD14^{high}$ $CD16^+$), and non-classical monocytes ($CD14^-$ $CD16^+$). The expressions of CD64, CD86, CD38, and HLADR can be evaluated to determine the activation state of the granulocytes, monocytes, and dendritic cells (DCs).

In panel 2, unconventional T cells and natural killer (NK) cells were identified. The mucosal-associated invariant T (MAIT) cells were identified by their $CD161^+$ TCR $V\alpha7.2^+$ phenotype in total T cells ($CD3^+$) and αβ cells. A gating strategy was applied to identify NK cells as $CD3^-$ $NKp46^+$ and classify them into early NK, effector NK, and terminal NK by CD16 and CD56. Additional two activating receptors (NKG2D and NKp46) distribution among different NK cell subsets were also evaluated.

T cell subsets were identified in panel 3–5. $CD4^+$ helper T (Th) cells were distinguished into Th1 ($CXCR3^+$ $CCR4^-$ $CCR6^-$), Th2 ($CXCR3^-$ $CCR4^+$ $CCR6^-$), Th9 ($CCR4^-$ $CCR6^+$), Th17 ($CXCR3^-$ $CCR4^+$ $CCR6^+$), and Th17Th1 ($CXCR3^+$ $CCR4^-$ $CCR6^+$). $CD8^+$ cytotoxic

T (Tc) cells were also identified based on the expression of CXCR3, CCR4, and CCR6 like Th cells. The regulatory T cells (Tregs) were identified by their $CD25^{high}$ $CD127^{-/low}$ phenotype on $CD4^+$ T cells. T cells at different stages of maturation were gated by CD45RA, CCR7, CD95. The expression of activation markers (CD69, CD28, HLADR, CD38) and inhibitory receptors (CD85j, PD-1, CD57) were used to determine the functional status of T cell subsets.

CD19 and CD20, two B cell pan markers were used to identified total B cells in panel 6. $CD11c^+$ B cells were regarded as memory B. Immunoglobulin (Ig) D, CD27, CD38, and CD24 were used to distinguish $CD27^+$ memory B cells, naïve B cells, transitional B cells, and founder B cells. Plasmablasts, plasma cells, and class-switched B cells were identified from IgD^- IgM^- B cells.

All antibodies for flow cytometric determinations were purchased from BioLegend and BD Biosciences (San Diego, CA, USA). Details were provided in Table S2.

Surface labeling for flow cytometry

Prior to staining, fluorescent antibody cocktails for each panel were pre-mixed in Stain buffer (PBS with 2% fetal bovine serum). Three staining protocols were used.

Staining Protocol 1: For panels 1, 2, 3, and 4, 100 μL of whole blood was incubated with 20 μL of antibody cocktails in 5 mL 12 × 75 mm polypropylene tubes at room temperature (RT, 20–25 °C) in the dark for 15 min 2 mL 1 × BD FACS Lysing Solution (BD Biosciences, catalog no. 349202) per tube was added and incubated at RT in the dark for 15 min. The lysed samples were centrifuged and washed once with 2 mL phosphate-buffered saline (PBS, Wisent, catalog no. 311-010-CL) at 500 g for 5 min at RT. Discard the supernatant and resuspend in a final volume of 250 μL 1% paraformaldehyde (PFA, Sangon Biotech, catalog no. A500684-0500). Store at 2–8 °C and protect from light until acquisition.

Staining Protocol 2: For panel 5, chemokine receptor antibody cocktails were first incubated at 37 °C in the dark for 15 min before being stained with surface antibody cocktails at RT for 15 min. The samples were then lysed, washed, and resuspended as described in Protocol 1, and store at 2–8 °C until acquisition.

Staining Protocol 3: For panel 6 (B cells panel), red blood cell lysis was performed first to minimize the effects of secreted immunoglobulins. After lysis and washing, 120 μL of antibody cocktails were added and incubated at RT in the dark for 15 min. Samples were washed and resuspended as described above, store at 2–8 °C, and protected from light until acquisition.

Sample loading and immune data acquisition

200 μL fixed cell suspension were collected for each sample on a five-laser Beckman Coulter CytoFLEX LX (Beckman Coulter, catalog no. C00446). Eight-peaks Rainbow Calibration Particles (Spherotech, catalog no. RCP-30-5A) and Anti-Mouse Ig, κ/Negative Control Compensation Particles (BD, catalog no. 552843) were used for instrument setup. Acquired data was analyzed using CytExpert_v2.4 (Beckman Coulter) and FlowJo_v10.8.1 (BD).

Immunophenotypes included the percentage of immune subsets in $CD45^+$ leukocytes and parent population (the upper level of the logical gating), and the median fluorescence intensity (MFI). The counts of immune subsets were calculated by combining the percentage of $CD45^+$ leukocytes with the white blood cell counts (WBC) measured by clinical routine blood tests.

Fecal sample treatment

DNA extraction and metagenomic sequencing

Total microbial genomic DNA from fecal samples was extracted using the TIANamp Stool DNA kit (TIANGEN, catalog no. GDP328-02). Metagenomic DNA samples were used to create Illumina sequencing libraries using the Tn5 DNA Library Prep Kit for Illumina (APExBIO, catalog no. K1802), followed by sequencing on the Illumina Novaseq6000 platform (2 × 150 base pairs). Quality control was conducted using KneadData (version 0.10.2), Trimmomatic (version 0.39),[15] and Bowtie2 (version 2.4.4).[16] Trimmomatic removed trimmed small non-human reads, while Bowtie2 filtered out human reads and rDNA reads by aligning them to the human reference genome (GRCh37) and SILVA 128 database. After quality control, an average of 64.7 million high-quality reads were obtained per sample, totaling approximately 9.6 GB of data.

Profiling of microbial taxa and functional potential

Taxonomic profiles were determined using MetaPhlan (version 3.0.13) with clade-specific marker genes.[17] The analysis was restricted to 135 species with a prevalence of at least 10% and a relative abundance of no less than 0.01%. Concurrently, functional profiles were executed with HUMAnN version 3.0.0, focusing on MetaCyc pathways and Enzyme Commission gene families (ECs).[18] The same filtering criteria as for microbial species were applied, resulting in the identification of 368 functional pathways and 1421 ECs.

Statistical analysis

Clinical characterization

The continuous variables were expressed as means and standard deviations, and Mann–Whitney U-tests were used to compare differences. The categorical variables were expressed as frequencies and percentages, and compared via Fisher's exact test. All results are shown in Table S1.

Multi-omics data

The Mann–Whitney U test was used to compare two groups by using the wilcox.test function in the R

package stats (v4.4.1), while for comparisons among three groups, Kruskal–Wallis test followed by Dunn's post hoc test with *P* value adjustment for pairwise comparisons was employed, using the kwAllPairsDunnTest function in the R package PMCMRplus (v1.9.12). All statistical tests were two-sided. All multiple comparisons were adjusted using the Benjamini-Hochberg method and an FDR below 0.20 was considered significant, consistent with previous studies.[19] The results of the single hypothesis testing were presented using nominal *P* values, with a *P* value of less than 0.05 was considered statistical significance. Effect size was used to measure the magnitude of the differences, and estimated by dividing the difference between estimated population means by the s.d. of control. Differential abundance analysis of metagenomic features was performed using Microbiome Multivariable Association with Linear Models (MaAsLin2, v1.14.1),[17] while alpha and beta diversity were assessed using the Shannon index and Bray–Curtis dissimilarity, respectively.

Spearman's rank correlation coefficient was utilized for correlation analysis to explore the relationships between metagenomic features, immune responses, and the clinical status of sepsis.[18] Mediation analysis was conducted to investigate the potential mediation effects among these variables using two regression models to estimate the indirect and direct effects, as implemented by the mediate function in the R package mediation (v4.5.0).[20] The mediator model on the associations between immune responses and independent variable (metagenomic features). The outcome model on the associations between outcome (sepsis) and both mediator (immune responses) and independent variable (metagenomic features). Bootstrapping procedures with 1000 Monte Carlo simulations were employed to estimate the proportional mediation effects. The diagnostic model included the most significant indicators of immunophenotypes, metagenomic phenotypes and clinical phenotypes. The Differential Expression Sliding Window Analysis (DE-SWAN) approach was employed to elucidate the dynamics of immunophenotypic alterations during hospitalization.[21] Survival analysis was conducted using Kaplan–Meier curves, and the significance of the differences between curves was determined using the log-rank test. A random forest model for sepsis-related mortality was developed using a random forest approach, with key immunophenotypic features identified through the Least Absolute Shrinkage and Selection Operator (LASSO) regression.[22] The model's predictive performance was evaluated using the area under the receiver operating characteristic (ROC) curve (AUC). All statistical analyses were conducted using R (v4.3.1) and RStudio (v2023.09.0–463).

Ethics approval

All recruitment, informed consent, and study procedures were approved by the Ethics Research Board of Zhongshan Hospital (Approval Number: B2022-107R). All participants or their legal representatives provided informed consent before joining the study.

Role of funders

The funders had no role in study design, data collection, data analyses, interpretation, or writing of this manuscript. All authors have full access to the data in the study and accept responsibility to submit for publication.

Results

Infection and inflammation were exhibited in sepsis

In our study, 31 septic patients, 25 non-septic ICU patients, and 18 healthy controls were enrolled. Compared with non-septic patients, septic patients had a similar distribution of age, gender, and BMI, as well as overall disease severity based on APACHE II scores, except for more pronounced organ failure according to SOFA scores (Table S1). Consistent with our expectation, septic patients exhibited elevated levels of procalcitonin (PCT), C-reactive protein (CRP), and neutrophil/lymphocyte ratios (NLR) compared with healthy controls or non-septic ICU patients, which indicated a bacterial infection profile (Fig. 1b, Table S1). All ICU patients, especially those with sepsis, demonstrated increased WBC and NLR, which suggested hyperinflammation.

Reduction of lymphocyte and reconfiguration of T cells reveal immunosuppression in sepsis

Compared with healthy controls, ICU patients demonstrated an increase in the relative percentage of neutrophils through a flow cytometric analysis of 74 whole blood samples (Fig. 1c, Fig. S2a). Immune cell subset comparisons revealed a greater disparity between sepsis and healthy controls than between non-sepsis and healthy controls (Fig. 1d), which indicated significant changes in immune cell composition in patients with sepsis.

The analysis of immune cell composition in sepsis revealed significant disruptions, particularly within lymphocyte subsets. Septic patients exhibited remarkable reductions in dendritic cells, basophils, and B cells compared with healthy controls (Fig. 1e, Fig. S2b), which highlighted impairments in both innate and adaptive immune responses. The differentiation and activation of $CD8^+$ T cells were notably suppressed, as indicated by an increased proportion of naïve $CD8^+$ T cells ($CD8^+$ T_N, $CD45RA^+$ $CCR7^+$ $CD95^-$) and a decreased proportion of effector $CD8^+$ T cells ($CD8^+$ T_E, $CD45RA^+$ $CCR7^-$) (Fig. 1f). Additionally, activated $CD8^+$ T cells ($CD8^+$ T_{Act}, $HLADR^+$ $CD38^+$) showed increased expression of PD-1 (Fig. 1g). An imbalance in the distribution of Th1 and Tregs within $CD4^+$ T cell populations was also observed (Fig. 1h), characterized by a decrease in pro-inflammatory Th1 cells and an increase

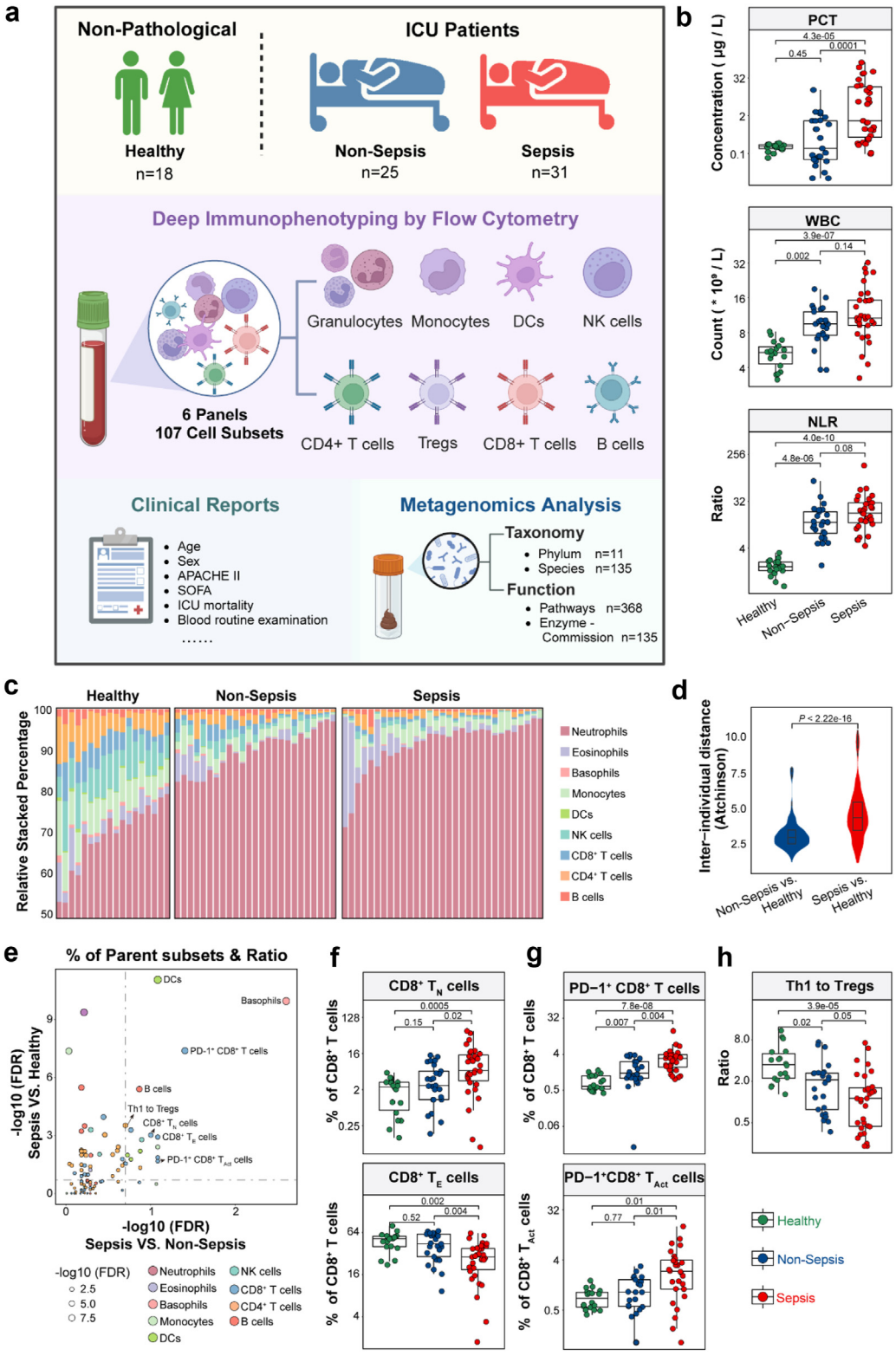

Fig. 1: **Study design and immune cell profiles. (a)** Schematic representation of the experimental workflow created with BioRender.com. **(b)** A comparative analysis of key clinical parameters, including PCT concentration, WBC count, and NLR across three groups (sepsis, n = 31; non-sepsis, n = 25; healthy, n = 18). FDR values shown in the graphs were calculated using Kruskal–Wallis test followed by Dunn's post hoc test

in anti-inflammatory Tregs (Fig. S2c). These findings together underscore the immunosuppressive state in sepsis, showing its characteristics of having a reduction in lymphocyte subsets and a reconfiguration of T cell subpopulations towards a functionally inhibited profile.

Sepsis and non-sepsis in ICU can be discriminated by NK cells and pDCs

The critical alterations in DCs and NK cells were revealed by the analysis of $CD45^+$ leukocyte subsets underscored immune dysregulation in septic patients (Fig. 2a). The reduction observed in both the proportions and absolute counts of NK and DCs subsets—including effector NK cells, early NK cells, pDCs, and mDCs (Fig. 2a and b, Fig. S2d)—pointed to a significant disruption in immune homeostasis. Moreover, the decreased expression of HLA-DR on pDCs and NKp46 on NK cells (Fig. 2c and d) highlighted the impaired functional capacity of innate immunity in sepsis. These findings emphasized that a compromised innate immune landscape in septic patients may contribute to their heightened susceptibility to infection and poor immune responsiveness.

In order to evaluate whether these indicators have clinical application value, ROC analysis was conducted to assess the diagnostic accuracy of immune cell phenotypes for distinguishing sepsis in ICU patients (Fig. 2e). The analysis revealed that the proportions of total NK cells and effector NK cells within $CD45^+$ leukocytes achieved robust diagnostic performance as demonstrated by an AUC of 0.861 (95% CI: 0.753–0.968). Similarly, early NK cells also showed high discriminatory power with an AUC of 0.849 (95% CI: 0.743–0.955). However, conventional infection markers, including CRP, PCT, and WBC, exhibited lower diagnostic efficacy. Notably, even the SOFA score, a widely used clinical assessment tool, yielded a comparatively modest AUC of 0.620 (95% CI: 0.535–0.705). Our results suggest that these immune cell markers, particularly NK cell subsets, may serve as more accurate and precise biomarkers compared with traditional clinical indicators, thereby highlighting their promise for improving sepsis diagnosis in clinical settings.

Combination of *Bacteroides salyersiae*, NK cells and CRP serve as an adjunctive tool for clinical diagnosis of sepsis

Metagenomic sequencing was employed to analyze the taxonomic and functional profiles of the gut microbiota in different populations across different groups (Fig. 3a), including 18 healthy controls, 10 non-septic ICU patients, and 13 septic patients. When compared with healthy individuals, both septic and non-septic ICU patients exhibited significantly reduced bacterial alpha diversity in the gut, and different microbial composition (Fig. 3a and b). The phylum-level distribution of gut microbiota was illustrated in Fig. 3c.

The MaAsLin2 analysis revealed differences in the abundance of four microbial species and their associated functional pathways between septic and non-septic ICU patients (Fig. 3d). Compared with healthy controls and non-septic ICU patients, septic patients exhibited significant alterations in 52 species from four phyla and 61 functional pathways, associated with immune signatures (Figs. S3 and S4).

*Clostridium clostridioforme*and and *Faecalibacterium prausnitzii* were enriched in non-sepsis, while *B. salyersiae* and *Enterococcus faecium* were more abundant in sepsis. Nine functional pathways associated with sepsis were identified (Fig. 3e), with the gut microbiome of sepsis showing a shift towards enhanced purine nucleotide and unsaturated fatty acid biosynthesis yet reduced glycogen and L-arginine biosynthesis. *B. salyersiae* and *E. faecium* contributed to these sepsis-enriched pathways (Fig. 3e).

B. salyersiae and the purine nucleotide biosynthesis pathway were negatively correlated with NK cell proportion and the HLADR expression on DCs (Fig. 3e and f). In addition, NK cell proportion and HLADR on pDCs statistically mediated the association between metagenomic profiles and sepsis (Fig. 3g, Fig. S5), which suggested a consistent finding with previous studies that dysbiosis in microbiota may trigger sepsis and lead to peripheral immune system dysregulation.[23]

We investigated the association of the combined metagenomics and immune responses with sepsis. The most significant indicators of sepsis were *B. salyersiae* from the metagenomic profiles (Fig. S6), NK cells

with Benjamini-Hochberg adjustment. **(c)** The relative stacked percentage of 9 cell populations in 74 blood samples sorted by group (sepsis, n = 31; non-sepsis, n = 25; healthy, n = 18). **(d)** Inter-individual variability in immune cell composition is quantified using Aitchison's distance, contrasting septic patients (n = 31) against healthy controls (n = 18) and non-septic patients (n = 25) against healthy controls (n = 18). *P* values calculated by Mann–Whitney U-test. **(e)** Comparison of immune features derived from each leukocyte subpopulation between experimental groups. Each dot represents one immunological feature; colors represent the leukocyte compartment. Dots above the horizontal dashed line represent features showing significant differences between the sepsis (n = 31) and healthy (n = 18). Dots to the right of the vertical dashed line represent features with significant differences between the sepsis (n = 31) and non-sepsis (n = 25). The FDR values were calculated by Mann–Whitney U-test with Benjamini-Hochberg adjustment, and differences were considered significant when FDR <0.20. **(f–h)** Boxplots display the alterations of T cell subsets across three groups (sepsis, n = 31; non-sepsis, n = 25; healthy, n = 18). FDR values shown in the graphs were calculated using Kruskal–Wallis test followed by Dunn's post hoc test with Benjamini-Hochberg adjustment. PCT, Procalcitonin; WBC, white blood cell; NLR, neutrophil-to-lymphocyte ratio; FDR, false discovery rate.

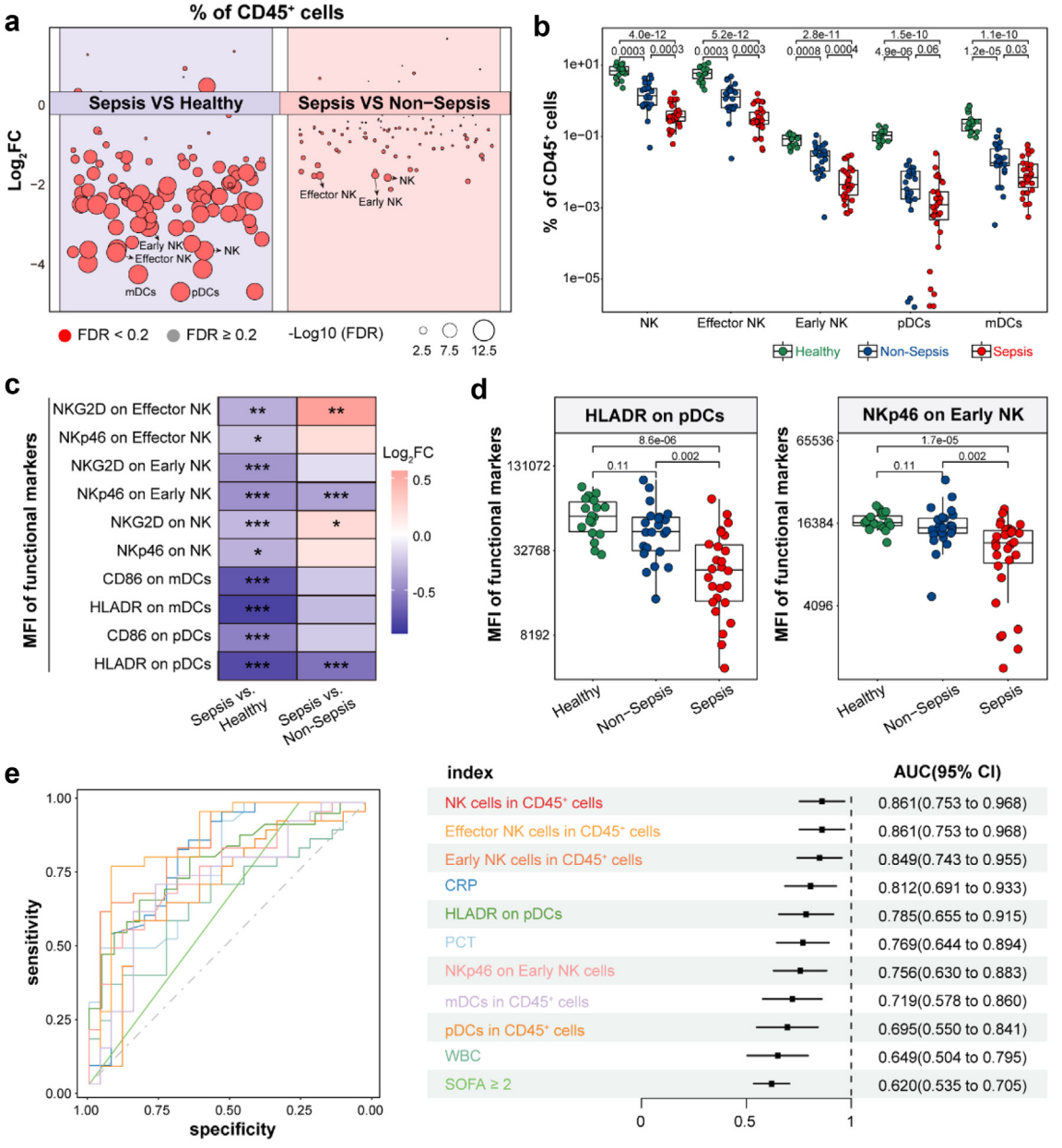

Fig. 2: **Distinguishing immune features between septic and non-septic patients. (a)** Comparisons of immune subsets between sepsis (n = 31) and non-sepsis (n = 25), as well as between sepsis (n = 31) and healthy participants (n = 18). Statistical analysis was conducted using Mann–Whitney U-test with Benjamini-Hochberg adjustment, and significance is denoted by red for FDR <0.20, with grey indicating FDR ≥0.20, and the size of the point corresponds to -Log10 (FDR). **(b)** Frequencies of NK cells and DCs across three groups (sepsis, n = 31; non-sepsis, n = 25; healthy, n = 18). FDR values shown in the graphs were calculated using Kruskal–Wallis test followed by Dunn's post hoc test with Benjamini-Hochberg adjustment. **(c)** Heatmap showing the $\log_2$FC in the MFI of functional markers on NK cells and DCs. Mann–Whitney U-test with Benjamini-Hochberg adjustment was used for comparisons between sepsis (n = 31) and non-sepsis (n = 25) or healthy (n = 18). **(d)** Boxplots displaying the alterations of MFI of HLADR on DCs and NKp46 on early NK cells across three groups (sepsis, n = 31; non-sepsis, n = 25; healthy, n = 18). FDR values shown in the graphs were calculated using Kruskal–Wallis test followed by Dunn's post hoc test with Benjamini-Hochberg adjustment. **(e)** ROC analysis shows the performance of immune phenotypes and clinical parameters in differentiating septic patients from non-septic patients. FDR, false discovery rate; NK, natural killer; DC, dendritic cells; FC, fold change; MIF, median fluorescence intensities; HLADR, human leukocyte antigen-DR; ROC, receiver operating characteristic. *FDR <0.20; **FDR <0.05; ***FDR <0.01.

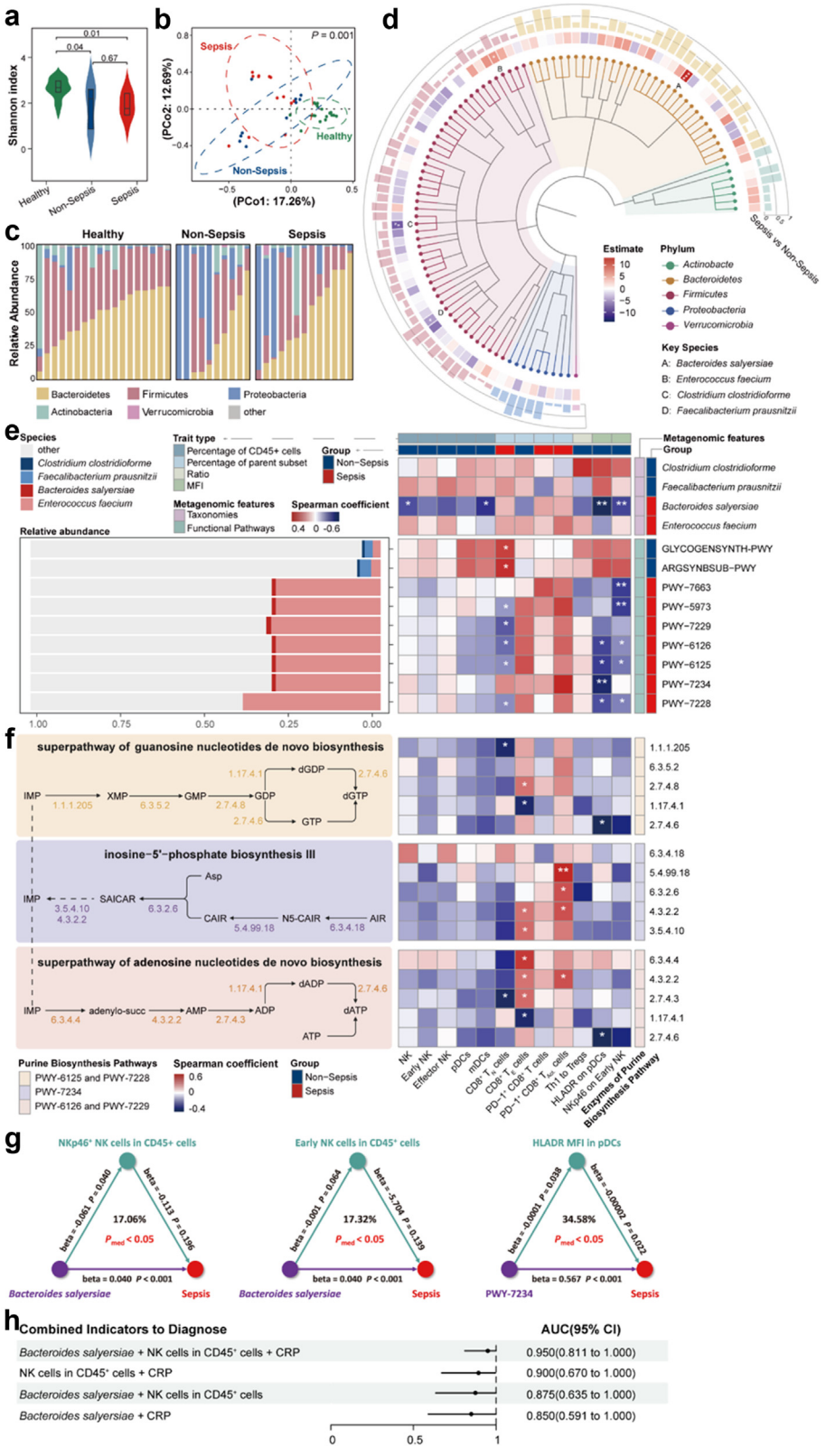
a
Shannon index
Healthy
Non-Sepsis
Sepsis
b
Sepsis
Healthy
Non-Sepsis
P = 0.001
(PCo2: 12.69%)
(PCo1: 17.26%)
c
Healthy
Non-Sepsis
Sepsis
Relative Abundance
Bacteroidetes
Firmicutes
Proteobacteria
Actinobacteria
Verrucomicrobia
other
d
Estimate
Phylum
Actinobacte
Bacteroidetes
Firmicutes
Proteobacteria
Verrucomicrobia
Key Species
A: Bacteroides salyersiae
B: Enterococcus faecium
C: Clostridium clostridioforme
D: Faecalibacterium prausnitzii
Sepsis vs Non-Sepsis
e
Species
other
Clostridium clostridioforme
Faecalibacterium prausnitzii
Bacteroides salyersiae
Enterococcus faecium
Trait type
Percentage of CD45+ cells
Percentage of parent subset
Ratio
MFI
Group
Non−Sepsis
Sepsis
Metagenomic features
Taxonomies
Functional Pathways
Spearman coefficient
Relative abundance
Metagenomic features
Group
Clostridium clostridioforme
Faecalibacterium prausnitzii
Bacteroides salyersiae
Enterococcus faecium
GLYCOGENSYNTH-PWY
ARGSYNBSUB-PWY
PWY-7663
PWY-5973
PWY-7229
PWY-6126
PWY-6125
PWY-7234
PWY-7228
f
superpathway of guanosine nucleotides de novo biosynthesis
IMP
XMP
GMP
GDP
GTP
dGDP
dGTP
inosine−5'−phosphate biosynthesis III
Asp
IMP
SAICAR
CAIR
N5-CAIR
AIR
superpathway of adenosine nucleotides de novo biosynthesis
IMP
adenylo-succ
AMP
ADP
ATP
dADP
dATP
Purine Biosynthesis Pathways
PWY-6125 and PWY-7228
PWY-7234
PWY-6126 and PWY-7229
Spearman coefficient
Group
Non−Sepsis
Sepsis
NK
Early NK
Effector NK
pDCs
mDCs
CD8+ Tc cells
CD8+ Tc cells
PD-1+ CD8+ Tc cells
PD-1+ CD8+ Tex cells
Th1 to Tregs
HLADR on pDCs
NKp46 on Early NK
Enzymes of Purine Biosynthesis Pathway
g
NKp46+ NK cells in CD45+ cells
17.06%
Pmed < 0.05
beta = 0.040 P < 0.001
Bacteroides salyersiae
Sepsis
Early NK cells in CD45+ cells
17.32%
Pmed < 0.05
beta = 0.040 P < 0.001
Bacteroides salyersiae
Sepsis
HLADR MFI in pDCs
34.58%
Pmed < 0.05
beta = 0.567 P < 0.001
PWY-7234
Sepsis
h
Combined Indicators to Diagnose
AUC(95% CI)
Bacteroides salyersiae + NK cells in CD45+ cells + CRP
0.950(0.811 to 1.000)
NK cells in CD45+ cells + CRP
0.900(0.670 to 1.000)
Bacteroides salyersiae + NK cells in CD45+ cells
0.875(0.635 to 1.000)
Bacteroides salyersiae + CRP
0.850(0.591 to 1.000)

within CD45$^+$ leukocytes from the immunophenotypes (Fig. 2e), and CRP as a clinical biomarker (Fig. 2e) based on single analysis. Notably, the model integrating all three indicators demonstrated superior discriminative power (AUC = 0.950, 95% CI: 0.811–1.000, Fig. 3h) compared with each indicator alone or paired combination (all AUC <0.875), which suggested that the onset of sepsis is linked to the dysregulation of multiple physiological systems.

The immunosuppressive phenotypes of sepsis contribute to the subtyping of septic patients

To assess the clinical relevance of immune cell phenotypes in sepsis, we performed Spearman's correlation analysis to examine their relationship with APACHE II and SOFA scores. The results revealed significant correlations, highlighting the profound impact of sepsis severity on immune dynamics. For APACHE II scores, lymphocyte subsets, including Th1 cells and CD8$^+$ T cells, demonstrated a significant negative correlation (Fig. S7a), whereas the proportion of Tregs within CD4$^+$ T cells showed a positive correlation. Similarly, for SOFA scores, a reduction in Tc2 and Th2 cell proportions was associated with higher scores (Fig. S7a), suggesting that sepsis-induced immunosuppression becomes more pronounced as the severity of sepsis increases. These findings underline the dynamic shift in immune cell behavior with worsening clinical outcomes.

To further quantify the relationship between immune phenotypes and sepsis severity, DE-SWAN was employed to evaluate the correlations with APACHE II scores (Fig. 4a) and SOFA scores (Fig. S7b). We identified a threshold APACHE II score of 21 as a critical point marking substantial immune phenotype alterations and a significant shift in immune cell behavior. If their APACHE II scores were ≥21, the patients were classified as severe sepsis cases (n = 12), while those with scores <21 were categorized as mild sepsis (n = 19). Results showed that severe sepsis, as indicated by an APACHE II score ≥21, was associated with a significantly higher mortality rate (75% vs. 26%, P = 0.012; Fig. 4b) and a greater incidence of septic shock (83% vs. 21%, P = 0.001; Fig. S7c). Furthermore, patients with severe sepsis exhibited significantly reduced survival rates, both at 28 days (P = 0.0095; Fig. 4c) and during their hospital stay (P = 0.032; Fig. S7d).

Peripheral blood leukocyte subset analysis further demonstrated that patients with severe sepsis had significantly reduced lymphocyte proportions, including NK cells, T cells, and B cells, particularly in those with poor prognoses (Fig. 4d). The percentage of lymphocytes among CD45$^+$ cells (Fig. 4e) and the absolute lymphocyte counts (Fig. S7e) were notably lower in severe septic patients, which underscored that lymphopenia may help to predict sepsis severity.

In addition, we evaluated immune cell subset proportions and ratios to capture changes in immune function. In severe septic patients, we observed a significant decrease in the Th1 to Treg ratio, suggesting a shift toward reduced inflammation and enhanced immune suppression (Fig. 4f and g). Moreover, the NLR was also significantly elevated in severe sepsis, despite similar neutrophil levels between mild and severe cases (Fig. S7f), which further highlighted the immune dysregulation in severe sepsis.

Immunophenotypes associated with sepsis severity enhance the predictive accuracy of clinical scores for prognosis

Our analysis revealed that the immune profiles of patients with severe sepsis closely resemble those of poor outcomes. To further assess the prognostic value of immune phenotypes in sepsis, we selected ten immune indicators that exhibited significant differences between severe and mild septic patients based on effect size (Fig. 5a). We applied LASSO regression to select variables from these ten indicators, retaining only those selected in at least 800 out of 1000 regression iterations (Fig. S8a). Ultimately, four immune indicators—lymphocytes in CD45$^+$ cells, Th17 cells in CD45$^+$ cells, CD4$^+$ T_{EM} cells in CD45$^+$ cells, and Th1 cells in CD45$^+$ cells—were selected to construct an immune model for

Fig. 3: **Metagenomic features of septic patients and their association with immune signatures. (a)** The violin plot indicating differences in bacterial alpha diversity (Shannon index) at the species level among healthy controls (n = 18), non-septic ICU patients (n = 10), and septic patients (n = 13). FDR values shown in the graphs were calculated using Kruskal–Wallis test followed by Dunn's post hoc test with Benjamini-Hochberg adjustment. **(b)** The scatter plot displaying the beta diversity among samples (sepsis, n = 13; non-sepsis, n = 10; healthy, n = 18) using Bray–Curtis distance. The P value indicates the PERMANOVA significance for intergroup comparisons. **(c)** Stacked bar plots illustrating the phylum-level distribution of gut microbiota across different samples (sepsis, n = 13; non-sepsis, n = 10; healthy, n = 18) based on metagenomic data. **(d)** Phylogenetic tree of key microbial species. The middle heatmap shows the MaAsLin2 analysis results for the microbial species among healthy controls (n = 18), non-septic ICU patients (n = 10), and septic patients (n = 13). The four key sepsis-associated species are marked with letters. The outer rings indicate the prevalence of each microbial species. **(e)** The horizontal bar plot (left) showing the contribution of key species to microbial functional pathways associated with sepsis (FDR-adjusted P < 0.2). The heatmap (right) denoting associations between key metagenomic features and immune signatures. **(f)** The key enzymes within the pathways of purine biosynthesis (left) and their association with immune signatures (right). **(g)** Mediation analysis of immune signatures on the association between metagenomic features and sepsis. The proportions of mediation are shown in the center. **(h)** The effect of multi-omics indicators on diagnosis of sepsis evaluated by random forest model. PERMANOVA, permutational multivariate analysis of variance; MaAsLin2, Microbiome Multivariable Association with Linear Models. *FDR <0.20; **FDR <0.05; ***FDR <0.01.

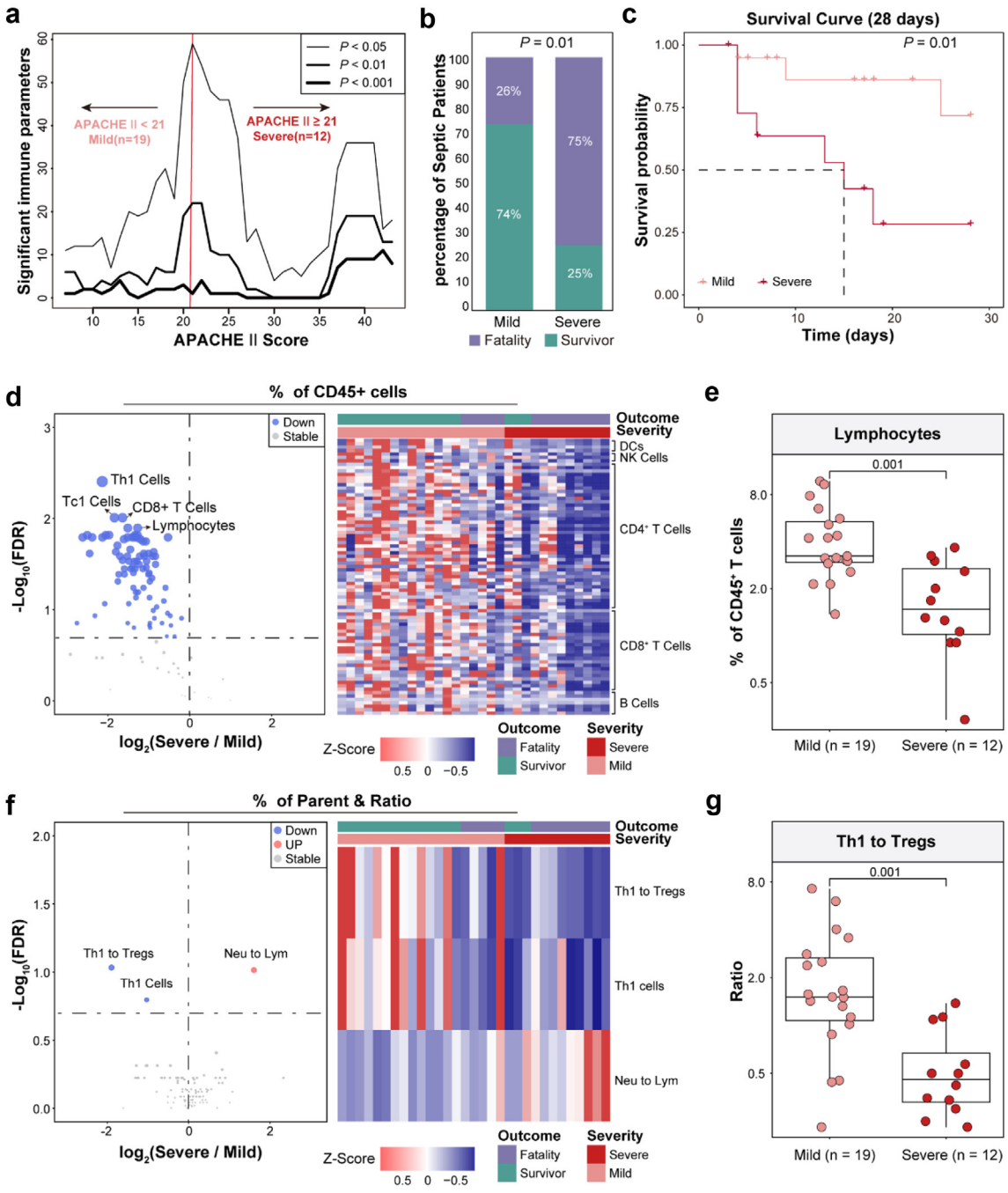

Fig. 4: **Distinguishing immune features between septic and non-septic patients. (a)** The number of immune features significantly changed by the APACHE II score. DE-SWAN identified a local peak at an APACHE II score of 21, which facilitated the classification of septic patients into Mild (n = 19) and Severe (n = 12). **(b)** Column diagram displaying the mortality rate of septic patients in Mild (n = 19) and Severe (n = 12). *P* value was calculated by Fisher's exact test. **(c)** Kaplan–Meier 28-day survival curves for Mild (n = 19) versus Severe (n = 12) cases. *P* value is based on the log-rank test. **(d)** Volcano plot and heatmap revealing the differential proportions of immune cell subsets within $CD45^+$ leukocytes between Mild (n = 19) and Severe (n = 12) patients. Significance was determined by Mann–Whitney U-test with Benjamini-Hochberg adjustment. Blue indicates depleted immune subsets, with the gray horizontal dashed line denoting a cutoff FDR of <0.20. **(e)** Quantification of lymphocyte count between mild (n = 19) and severe (n = 12) samples. *P* value was calculated by Mann–Whitney U-test. **(f)** Volcano plot and heatmap showing differential proportions of immune cell subsets within their parent populations and ratio values between Mild (n = 19) and Severe (n = 12). Significance was determined by Mann–Whitney U-test with Benjamini-Hochberg adjustment. Blue and red indicate

predicting 28-day mortality in septic patients (Fig. 5b). Moreover, clinical scores such as APACHE II and SOFA were found to correlate with patient prognosis, with higher scores in deceased patients and lower scores in those who survived (Fig. 5c).

A random forest model was subsequently developed using 60% of sepsis patient data for training and the remaining 40% for validation. The results demonstrated that all four immune indicators outperformed clinical scores in predicting sepsis outcomes, with the proportion of lymphocytes in $CD45^+$ cells exhibiting the highest AUC of 0.810 (95% CI: 0.652–0.967) (Fig. S8b). The inclusion of the four key immune indicators significantly improved the accuracy of prognosis prediction, achieved an AUC of AUC of 0.906 (95% CI: 0.732–1.000) (Fig. 5d), and was further enhanced when combined with clinical scores (AUC = 0.938, 95% CI: 0.796–1.000). The ranking of these six indicators in the combined model emphasized the importance of immune phenotypes in predicting sepsis prognosis (Fig. 5e). Notably, the combined model was able to predict sepsis mortality that cannot be captured by clinical scores alone. For instance, despite an APACHE II score indicating mild sepsis, the composite model that incorporated both immune indicators and clinical scores, successfully predicted mortality (Fig. 5f). This finding underscores the necessity of combining immune phenotypes with clinical scores for a more comprehensive assessment of sepsis prognosis.

Discussion

The current study investigated the relationship between peripheral blood immune cell characteristics, gut microbiota disturbance, and sepsis in adult ICU patients through a comparison with non-septic critically ill patients or healthy controls by integrating high-throughput flow cytometry and metagenomic sequencing. We characterized distinctive patterns of immune dysregulation in septic patients, including increased neutrophil counts (neutrophilia), decreased lymphocyte populations (lymphopenia), substantial remodeling of T cell subsets, reduced NK cell frequencies, and diminished HLADR expression on myeloid cells. These immune disturbances not only statistically mediated the association between gut microbiota alterations and sepsis, but also more importantly, demonstrated higher diagnostic accuracy and prognostic value compared with conventional clinical markers.

Consistent with previous studies, our findings further support the simultaneous occurrence of excessive inflammation and immune suppression in sepsis.[24–27] Compared with controls, septic patients exhibited remarkably elevated levels of CRP, WBC, neutrophil counts, and NLR, which indicated a pronounced organ damage in sepsis.[28,29] In contrast, a significant reduction in the number and proportion of most immune cell populations was observed, excluding neutrophils, with lymphocytes being particularly diminished. Additionally, the expression of HLADR on monocytes and DCs was significantly downregulated, while the proportion of Tregs was markedly increased. Furthermore, the upregulation of PD-1, a marker associated with immune cell exhaustion,[30] was evident in a greater proportion of T cells. Overall, our study highlights the distinct immunological dysregulation in septic patients, and characterizes it by a neutrophil-driven hyperinflammatory response and concurrent immune suppression, particularly in non-neutrophilic cell subsets.

Interestingly, our study observed a downregulation of NKp46 and NKG2D expression on NK cells, a finding that aligns with the results of Chiche et al. that impaired NK cell cytotoxicity and reduced expression of NKp30 and NKp46 in septic patients.[31] As key components of the innate immune system, NK cells play a crucial role in the early immune response to pathogen invasion,[32] which underscores their potential as diagnostic markers for sepsis in its initial stages. Our data support this hypothesis and demonstrate that NK cell subsets exhibited higher diagnostic accuracy for distinguishing ICU patients with sepsis from non-sepsis individuals when compared with current clinical biomarkers such as CRP, PCT, and the SOFA score.

As a proof-of-concept study, our data demonstrate that immune phenotyping could serve as a complement to existing scoring systems like SOFA and APACHE II, aiding clinicians in identifying high-risk patients. By providing immunological candidate markers for conducting adjunctive diagnostic tests and identifying a key point in the variation of immune profiles with disease severity, our study may guide the initiation and de-escalation of antibiotic therapy. This finding is consistent with the perspective of Parlato and Cavaillon, who found that host response markers may help to guide antibiotic treatment and reduce resistance.[33] By leveraging the diagnostic power of these combined markers, clinicians can make more informed decisions, which may ultimately lead to improved patient outcomes and antimicrobial stewardship.

Our findings reveal that immune phenotypes provide crucial complementary information for patient stratification and outcome prediction, though clinical severity

depleted and increased immune subsets, respectively, with the gray horizontal dashed line denoting a cutoff FDR of <0.20. **(g)** Boxplots showing the Th1 to Tregs ratio, exhibiting significant differences between Mild (n = 19) and Severe (n = 12) samples. *P* value was calculated by Mann–Whitney U-test. APACHE, Acute Physiology and Chronic Health Evaluation; DE-SWAN, Differential expression sliding window analysis; FDR, false discovery rate; Th, Helper T.

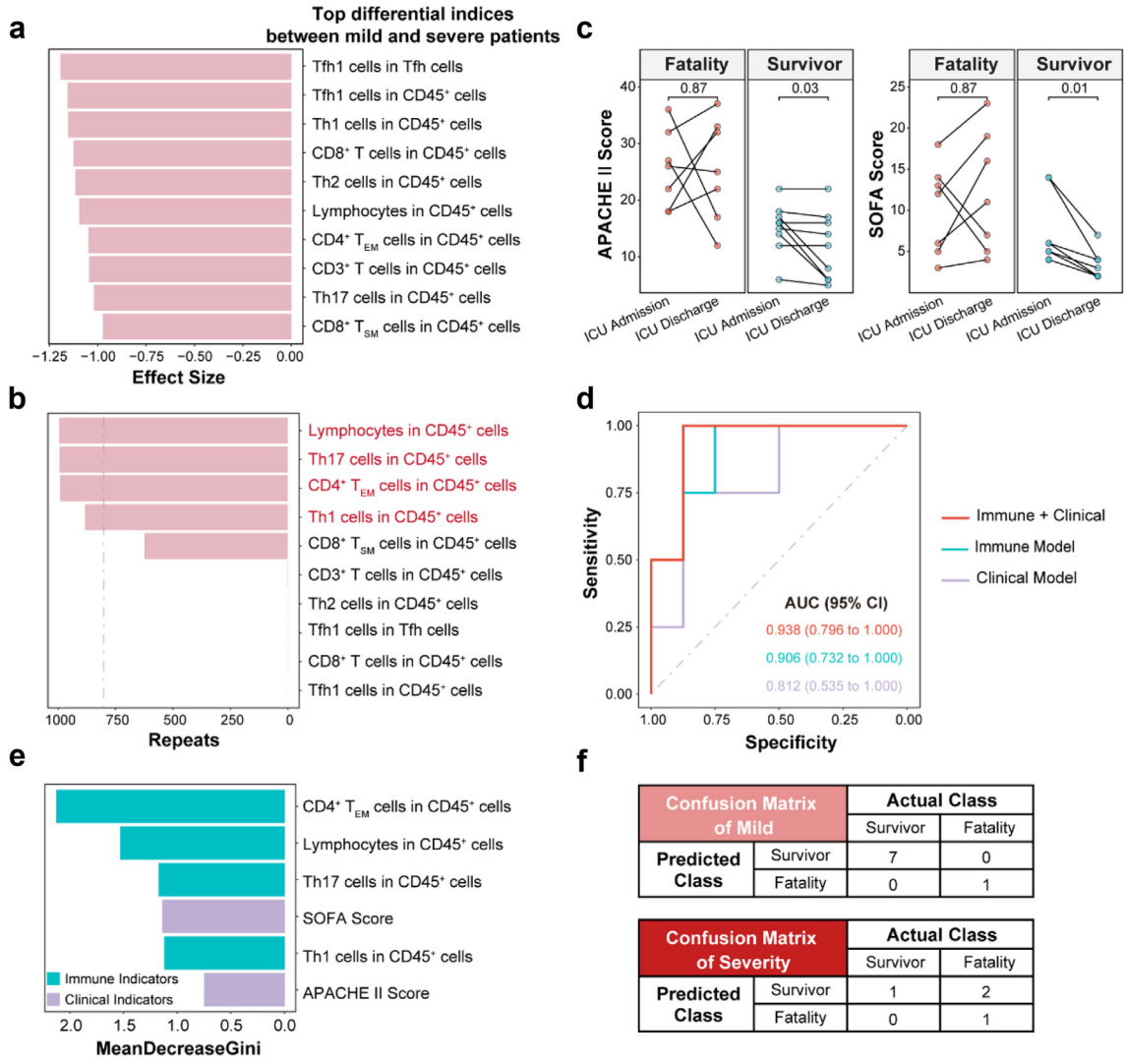

Fig. 5: **Construction of prognostic models by immunophenotypes and clinical scores. (a)** Top ten indicators identified by effect size between Mild (n = 19) and Severe (n = 12) cases. **(b)** 4 indicators without multicollinearity are strongly associated with fatality in sepsis by LASSO regression analysis. **(c)** The trends of APACHE II and SOFA scores during ICU admission among septic patients with different prognoses (Fatality, n = 7; Survivor, n = 9). *P* values were calculated by paired Mann–Whitney U-test. **(d)** Performance of the random forest models showed the highest prognostic accuracy in testing set (n = 12) when combined immunophenotypes and clinical scores evaluated by AUC. **(e)** Ranking of the importance of included indicators in the combination model. **(f)** The confusion matrix of the combination model. LASSO, Least Absolute Shrinkage and Selection Operator; APACHE, Acute Physiology and Chronic Health Evaluation; SOFA, Sequential Organ Failure Assessment; ICU, Intensive Care Unit; AUC, the area under the receiver operating characteristic curve.

scores such as SOFA and APACHE II remain fundamental tools for prognostic evaluation in sepsis, providing an alternative to address the challenge of lack of accuracy in predicting sepsis outcomes in current clinical practice.[34,35] Through comprehensive immune profiling, we identified four key immune indicators that significantly enhance prognostic accuracy when combined with traditional clinical scores, which are lymphocyte proportion in $CD45^+$ cells, Th17 cells in $CD45^+$ cells, $CD4^+$ T_{EM} cells in $CD45^+$ cells, and Th1 cells in $CD45^+$ cells, respectively. The combination of immune parameters and clinical severity scores in the assessment enables clinicians to identify high-risk patients who might be overlooked by traditional scoring systems alone, which is particularly crucial for patients with seemingly mild clinical scores yet compromised immune function, because they may require more intensive monitoring and aggressive therapeutic interventions. Moreover, this integrated approach provides a more nuanced understanding of sepsis

heterogeneity, potentially guiding personalized treatment strategies based on both clinical severity and immune status.

In addition, we found consistently increased CCR7 expression on $CD4^+$ and $CD8^+$ T cells in patients with sepsis, as evidenced by the increased proportion of naïve T cells ($CCR7^+$ $CD45RA^+$ $CD95^-$). This finding suggests potential alterations in T cell trafficking in septic patients. The ingress and egress of lymphocytes from lymph nodes to the bloodstream are tightly controlled by cell-intrinsic clock genes and extrinsic glucocorticoids through the regulation of chemokine receptor CCR7 expression.[36–38] According to recent studies, the observed increase in CCR7 expression and the proportion of naïve T cells in septic patients may result from dysregulation of the hypothalamic-pituitary-adrenal (HPA) axis and elevated free cortisol levels, which could induce CCR7 expression, promote T cell redistribution, and contribute to lymphopenia.[39,40] However, they did not directly investigate the underlying mechanisms responsible for the increased CCR7 expression in septic patients, entailing further research of the contributive factors such as the potential role of the HPA axis, cortisol levels, and other immunomodulatory pathways. Future studies should focus on elucidating the precise mechanisms driving the observed alterations in T cell trafficking and their implications for sepsis-related immune dysfunction.

Our study introduces immune profiling as a potential diagnostic tool for sepsis by offering easily detectable biomarkers with significant clinical implications. Specifically, we observed a significant decrease of NK cells in $CD45^+$ leukocytes, which supports the idea that NK cell subsets may serve as more accurate diagnostic markers for sepsis than current clinical biomarkers such as CRP, PCT, and the SOFA score. Additionally, we integrated immune phenotyping with clinical scoring systems to classify sepsis severity, demonstrating its potential to complement SOFA and APACHE II scores. Furthermore, we identified key T cell subsets that predict sepsis prognosis, offering valuable insights beyond traditional severity scores. By combining immune profiling with clinical scores, we can better stratify patients, particularly by providing patients who have mild clinical scores yet impaired immune function with more personalized treatment strategies.

Furthermore, this study uniquely associates peripheral blood immunophenotypes with metagenomic features in sepsis, offering preliminary insights into the potential biological significance of their interactions. Our findings suggest that NK cell subsets statistically mediate the relationship between *B. salyersiae* and sepsis, implying possible mechanisms underlying sepsis pathogenesis and identifying potential targets for intervention. As growing evidence indicates a bidirectional interplay between the immune system and gut microbiota in health and disease,[41] our study has employed metagenomic sequencing instead of 16 S rRNA sequencing to extend the prior studies that identified the enrichment of genera such as *Klebsiella*, *Enterococcus*, and *Bacteroides* in septic patients and their association with adverse clinical outcomes,[11,42–46] providing higher-resolution species-level insights. Beneficial bacteria such as *C. clostridioforme* and *F. prausnitzii*, enriched in the non-septic patients, are known for their anti-inflammatory properties.[47,48] Septic patients exhibited reduced gut microbiota diversity, which has been associated with worse outcomes and decreased survival rates.[49] In our study, *B. salyersiae* and *E. faecium* were enriched in sepsis. Among them, *E. faecium* is a pathogenic bacterium associated with critical illness,[50] while *B. salyersiae*, a commensal gut bacterium capable of degrading polysaccharides,[51] also exhibits opportunistic pathogenicity under certain conditions, such as ulcerative colitis.[52] In addition, *B. salyersiae* was found in the bronchoalveolar lavage specimens from patients with sepsis and acute respiratory distress syndrome, where it was positively correlated with Tumor necrosis factor-α,[53] and inversely associated with T lymphocytes and natural killer cells.[23] Furthermore, abnormal accumulation of *B. salyersiae* may contribute to the development of diffuse large B-cell lymphoma and peripheral immune dysfunction.[23] While prior studies have reported associations between *B. salyersiae* and immune function, its relationship with sepsis has been rarely addressed. Our analysis employs random forest modeling, which allowed us to identify key microbiota species, immunophenotype, clinical factor, and their relationships with sepsis outcomes which can guide clinical decisions in sepsis and improve patient outcomes.[14]

Although our study is the largest to date integrating immunome and gut microbiome analysis in sepsis research, it is still limited in sample size. Future studies with larger sample sizes are needed to validate the biomarkers identified for stratifying sepsis risk. In addition, incorporating multi-center samples will enhance the generalizability of our findings. The collection of fecal samples from ICU patients presented practical challenges due to altered bowel movements in critical illness; future studies might benefit from alternative sampling methods such as anal swabs to better characterize intestinal dysbiosis. Additionally, while our findings suggest important associations between gut microbiota and immune phenotypes, the causal relationships between these factors and their roles in sepsis pathogenesis may be further investigated. Future longitudinal studies may also build upon the foundation of this cross-sectional research to further elucidate the temporal dynamics of immune responses in sepsis development and prognosis.

In conclusion, our study identified distinct patterns of immune dysregulation in sepsis through comprehensive immunophenotyping and metagenomic

analysis. We demonstrated that NK cells from the innate immunity system, when combined with the appropriate gut *B. salyersiae* abundance and circulating CRP levels, serve as valuable diagnostic markers for sepsis. In addition, specific T cell subsets from adaptive immunity correlated with disease severity and predicted patient outcomes when integrated with clinical scores. By demonstrating the complementary role of immune markers to traditional clinical assessments and the interaction between gut microbiota and immune phenotypes, we provide new insights into sepsis pathogenesis and propose more precise diagnostic and prognostic strategies in sepsis management.

Contributors

YL, JG, YZ, FQ, and HH designed and coordinated the study. YL, JG, and HL participated in sample processing and data acquisition. YL, JG, XS, HL, YL, WQ, XH, JH, YZ, AZ, YZ, FQ, and HH completed the data analysis and results interpretation. YL, XS, YL, FQ and HH completed the first draft of the article. YL had full access to all the data in the study and verified the underlying data. All authors reviewed, revised, and approved the final manuscript.

Data sharing statement

The deidentified datasets used and/or analyzed during the current study are available from the corresponding author on reasonable request.

Declaration of interests

The authors declare that they have no conflict of interest.

Acknowledgements

We thank the medical and research teams at Zhongshan Hospital. We thank Huiqin Lin, Quanzhong Liu, Yun Wang, Jing Sun and Miaomiao Wang for their support in sample transportation, blood sample processing, and data collection. We thank the Human Phenome Data Center of Fudan University for their support. This project was supported by the National Key R&D Program of China (2023YFC2307600, 2021YFA1301000), Shanghai Municipal Science and Technology Major Project (2023SHZDZX02, 2017SHZDZX01), Shanghai Municipal Technology Standards Project (23DZ2202600).

Appendix A. Supplementary data

Supplementary data related to this article can be found at https://doi.org/10.1016/j.ebiom.2025.105586.

References

1 Singer M, Deutschman CS, Seymour CW, et al. The third international consensus definitions for sepsis and septic shock (Sepsis-3). *JAMA*. 2016;315(8):801–810.
2 Angus DC, Linde-Zwirble WT, Lidicker J, Clermont G, Carcillo J, Pinsky MR. Epidemiology of severe sepsis in the United States: analysis of incidence, outcome, and associated costs of care. *Crit Care Med*. 2001;29(7):1303–1310.
3 Rudd KE, Johnson SC, Agesa KM, et al. Global, regional, and national sepsis incidence and mortality, 1990-2017: analysis for the Global Burden of Disease Study. *Lancet*. 2020;395(10219):200–211.
4 Angus DC, van der Poll T. Severe sepsis and septic shock. *N Engl J Med*. 2013;369(9):840–851.
5 Li Y, Zhang H, Chen C, et al. Biomimetic immunosuppressive exosomes that inhibit cytokine storms contribute to the alleviation of sepsis. *Adv Mater*. 2022;34(19):e2108476.
6 van der Poll T, van de Veerdonk FL, Scicluna BP, Netea MG. The immunopathology of sepsis and potential therapeutic targets. *Nat Rev Immunol*. 2017;17(7):407–420.
7 Darden DB, Kelly LS, Fenner BP, Moldawer LL, Mohr AM, Efron PA. Dysregulated immunity and immunotherapy after sepsis. *J Clin Med*. 2021;10(8):1742.
8 Rubio I, Osuchowski MF, Shankar-Hari M, et al. Current gaps in sepsis immunology: new opportunities for translational research. *Lancet Infect Dis*. 2019;19(12):e422–e436.
9 Shi R, Wang J, Zhang Z, Leng Y, Chen AF. ASGR1 promotes liver injury in sepsis by modulating monocyte-to-macrophage differentiation via NF-kappaB/ATF5 pathway. *Life Sci*. 2023;315:121339.
10 Ahmed MGT, Limmer A, Hartmann M. CD45RA and CD45RO are regulated in a cell-type specific manner in inflammation and sepsis. *Cells*. 2023;12(14):1873.
11 Zhang Z, Cheng L, Ning D. Gut microbiota and sepsis: bidirectional Mendelian study and mediation analysis. *Front Immunol*. 2023;14:1234924.
12 Liu Y, Zhao H, Fu B, Jiang S, Wang J, Wan Y. Mapping cell phenomics with multiparametric flow cytometry assays. *Phenomics*. 2022;2(4):272–281.
13 Ikeda T, Nishida A, Yamano M, Kimura I. Short-chain fatty acid receptors and gut microbiota as therapeutic targets in metabolic, immune, and neurological diseases. *Pharmacol Ther*. 2022;239:108273.
14 Cajander S, Kox M, Scicluna BP, et al. Profiling the dysregulated immune response in sepsis: overcoming challenges to achieve the goal of precision medicine. *Lancet Respir Med*. 2024;12(4):305–322.
15 Bolger AM, Lohse M, Usadel B. Trimmomatic: a flexible trimmer for Illumina sequence data. *Bioinformatics*. 2014;30(15):2114–2120.
16 Langmead B, Salzberg SL. Fast gapped-read alignment with Bowtie 2. *Nat Methods*. 2012;9(4):357–359.
17 Segata N, Waldron L, Ballarini A, Narasimhan V, Jousson O, Huttenhower C. Metagenomic microbial community profiling using unique clade-specific marker genes. *Nat Methods*. 2012;9(8):811–814.
18 Beghini F, McIver LJ, Blanco-Míguez A, et al. Integrating taxonomic, functional, and strain-level profiling of diverse microbial communities with bioBakery 3. *Elife*. 2021;10:e65088.
19 Pu Y, Sun Z, Zhang H, et al. Gut microbial features and circulating metabolomic signatures of frailty in older adults. *Nat Aging*. 2024;4(9):1249–1262.
20 Tingley D, Yamamoto T, Hirose K, Keele L, Imai K. Mediation: R package for causal mediation analysis. *J Stat Software*. 2014;59(5):1–38.
21 Lehallier B, Gate D, Schaum N, et al. Undulating changes in human plasma proteome profiles across the lifespan. *Nat Med*. 2019;25(12):1843–1850.
22 Hu J, Szymczak S. A review on longitudinal data analysis with random forest. *Brief Bioinform*. 2023;24(2):bbad002.
23 Zhang Y, Han S, Xiao X, et al. Integration analysis of tumor metagenome and peripheral immunity data of diffuse large-B cell lymphoma. *Front Immunol*. 2023;14:1146861.
24 van der Poll T, Shankar-Hari M, Wiersinga WJ. The immunology of sepsis. *Immunity*. 2021;54(11):2450–2464.
25 Wiersinga WJ, van der Poll T. Immunopathophysiology of human sepsis. *eBioMedicine*. 2022;86:104363.
26 Steinhagen F, Schmidt SV, Schewe JC, Peukert K, Klinman DM, Bode C. Immunotherapy in sepsis - brake or accelerate? *Pharmacol Ther*. 2020;208:107476.
27 Torres LK, Pickkers P, van der Poll T. Sepsis-induced immunosuppression. *Annu Rev Physiol*. 2022;84:157–181.
28 Pierrakos C, Velissaris D, Bisdorff M, Marshall JC, Vincent JL. Biomarkers of sepsis: time for a reappraisal. *Crit Care*. 2020;24(1):287.
29 Liu HH, Zhang MW, Guo JB, Li J, Su L. Procalcitonin and C-reactive protein in early diagnosis of sepsis caused by either Gram-negative or Gram-positive bacteria. *Ir J Med Sci*. 2017;186(1):207–212.
30 Monneret G, Gossez M, Venet F. Sepsis in PD-1 light. *Crit Care*. 2016;20(1):186.
31 Chiche L, Forel JM, Thomas G, et al. The role of natural killer cells in sepsis. *J Biomed Biotechnol*. 2011;2011:986491.
32 Spits H, Bernink JH, Lanier L. NK cells and type 1 innate lymphoid cells: partners in host defense. *Nat Immunol*. 2016;17(7):758–764.
33 Parlato M, Cavaillon JM. Host response biomarkers in the diagnosis of sepsis: a general overview. *Methods Mol Biol*. 2015;1237:149–211.
34 Llitjos JF, Carrol ED, Osuchowski MF, et al. Enhancing sepsis biomarker development: key considerations from public and private perspectives. *Crit Care*. 2024;28(1):238.
35 Huang Y, Jiang S, Li W, Fan Y, Leng Y, Gao C. Establishment and effectiveness evaluation of a scoring system-RAAS (RDW, AGE,

APACHE II, SOFA) for sepsis by a retrospective analysis. *J Inflamm Res*. 2022;15:465–474.
36 Anderson BE, Taylor PA, McNiff JM, et al. Effects of donor T-cell trafficking and priming site on graft-versus-host disease induction by naive and memory phenotype CD4 T cells. *Blood*. 2008;111(10):5242–5251.
37 Sharma N, Benechet AP, Lefrancois L, Khanna KM. CD8 T cells enter the splenic T cell zones independently of CCR7, but the subsequent expansion and trafficking patterns of effector T cells after infection are dysregulated in the absence of CCR7 migratory cues. *J Immunol*. 2015;195(11):5227–5236.
38 Wang Q, Chu F, Zhang X, et al. Infectious bursal disease virus replication is inhibited by avain T cell chemoattractant chemokine CCL19. *Front Microbiol*. 2022;13:912908.
39 Jiang Y, Hu Y, Yang Y, et al. Tong-Xie-Yao-Fang promotes dendritic cells maturation and retards tumor growth in colorectal cancer mice with chronic restraint stress. *J Ethnopharmacol*. 2024;319(Pt 1):117069.
40 Langouche L, Teblick A, Gunst J, Van den Berghe G. The hypothalamus-pituitary-adrenocortical response to critical illness: a concept in need of revision. *Endocr Rev*. 2023;44(6):1096–1106.
41 Zheng D, Liwinski T, Elinav E. Interaction between microbiota and immunity in health and disease. *Cell Res*. 2020;30(6):492–506.
42 Mu S, Xiang H, Wang Y, et al. The pathogens of secondary infection in septic patients share a similar genotype to those that predominate in the gut. *Crit Care*. 2022;26(1):68.
43 Sun S, Wang D, Dong D, et al. Altered intestinal microbiome and metabolome correspond to the clinical outcome of sepsis. *Crit Care*. 2023;27(1):127.
44 Lankelma JM, van Vught LA, Belzer C, et al. Critically ill patients demonstrate large interpersonal variation in intestinal microbiota dysregulation: a pilot study. *Intensive Care Med*. 2017;43(1):59–68.
45 Liu W, Cheng M, Li J, et al. Classification of the gut microbiota of patients in intensive care units during development of sepsis and septic shock. *Dev Reprod Biol*. 2020;18(6):696–707.
46 Agudelo-Ochoa GM, Valdés-Duque BE, Giraldo-Giraldo NA, et al. Gut microbiota profiles in critically ill patients, potential biomarkers and risk variables for sepsis. *Gut Microb*. 2020;12(1):1707610.
47 Leonard MM, Valitutti F, Karathia H, et al. Microbiome signatures of progression toward celiac disease onset in at-risk children in a longitudinal prospective cohort study. *Proc Natl Acad Sci U S A*. 2021;118(29):e2020322118.
48 Sokol H, Pigneur B, Watterlot L, et al. Faecalibacterium prausnitzii is an anti-inflammatory commensal bacterium identified by gut microbiota analysis of Crohn disease patients. *Proc Natl Acad Sci U S A*. 2008;105(43):16731–16736.
49 Swarte JC, Li Y, Hu S, et al. Gut microbiome dysbiosis is associated with increased mortality after solid organ transplantation. *Sci Transl Med*. 2022;14(660):eabn7566.
50 Zhou X, Willems RJL, Friedrich AW, Rossen JWA, Bathoorn E. Enterococcus faecium: from microbiological insights to practical recommendations for infection control and diagnostics. *Antimicrob Resist Infect Control*. 2020;9(1):130.
51 Wang Y, Ma M, Dai W, Shang Q, Yu G. Bacteroides salyersiae is a potent chondroitin sulfate-degrading species in the human gut microbiota. *Microbiome*. 2024;12(1):41.
52 Zhang B, Magnaye KM, Stryker E, et al. Sustained mucosal colonization and fecal metabolic dysfunction by Bacteroides associates with fecal microbial transplant failure in ulcerative colitis patients. *Sci Rep*. 2024;14(1):18558.
53 Dickson RP, Singer BH, Newstead MW, et al. Enrichment of the lung microbiome with gut bacteria in sepsis and the acute respiratory distress syndrome. *Nat Microbiol*. 2016;1(10):16113.